

## CFD ANALYSES OF COMBUSTOR AND NOZZLE FLOWFIELDS

Hsin-Hua Tsuei<sup>†</sup> and Charles L. Merkle<sup>§</sup>  
Propulsion Engineering Research Center  
and

Department of Mechanical Engineering  
The Pennsylvania State University  
University Park, PA 16802

## SUMMARY:

The objectives of the present research are to improve design capabilities for low thrust rocket engines through understanding of the detailed mixing and combustion processes. A Computational Fluid Dynamic (CFD) technique is employed to model the flowfields within the combustor, nozzle and near plume field. The computational modeling of the rocket engine flowfields requires the application of the complete Navier-Stokes equations, coupled with species diffusion equations. Of particular interest is a small gaseous hydrogen-oxygen thruster which is considered as a coordinated part of a on-going experimental program at NASA LeRC. The numerical procedure is performed on both time-marching and time-accurate algorithms, using an LU approximate factorization in time, flux split upwinding differencing in space. The integrity of fuel film cooling along the wall, its effectiveness in the mixing with the core flow including unsteady large scale effects, the resultant impact on performance and the assessment of the near plume flow expansion to finite pressure altitude chamber is addressed.

## TECHNICAL DISCUSSION:

Propulsion related flowfields are characterized by a wide variety of physical phenomena. In the rocket engine combustion chamber, mixing and combustion processes between the fuel and oxidizer result in regions of strong heat release and species generation. The present paper addresses a small gaseous  $H_2/O_2$  engine in which about 60% of the fuel is used for film cooling. The velocity and molecular weight differences in these two streams suggest the likelihood that large scale vortices are present in the resulting shear layer. Downstream of the combustor, the flow accelerates from low subsonic to supersonic speed through a convergent-divergent nozzle. The Mach number increases rapidly because of the increasing flow speed, while the chemical reaction processes slow down and the heat release is small. In the supersonic portion of the nozzle, the flow is essentially frozen. A computational model that is capable of calculating reacting flows at both subsonic and supersonic speed is of immediate interest.

Although the application of reactive Navier-Stokes equations to rocket engines is appropriate for all engine sizes, the primary near-term usage is for low thrust, auxiliary propulsion engines [1-7]. Accurate numerical predictions of global performance and local flowfields in these small motors require detailed consideration of the mixing, viscous diffusion, species generation and heat release associated with the combustion processes. Small engines are characterized by low Reynolds numbers and therefore the wall boundary layer occupies a significant portion of the combustor. The specific engine we consider in the current research is a gaseous hydrogen-oxygen engine designed for NASA LeRC to provide auxiliary propulsion and attitude control for the Space Station freedom [1]. This small engine provides about 110 N (25 lbf) of thrust.

---

<sup>†</sup> Graduate Research Assistant

<sup>§</sup> Distinguished Alumni Professor

Previous research has been done both experimentally [2-4] and numerically [5-7] for these types of engines. Comparisons have shown qualitative agreement [5-7] but some important physics must be included in the computational model in order to provide more accurate engine performance prediction and local flowfield characteristics. Engine global performance parameters such as thrust and specific impulse have been consistently underpredicted [5,6] by 4 %, despite the fact that ideal combustion was assumed in the numerical modeling of the core flow. Further, comparisons with detailed local flowfield point data measurement in the near plume region have been made by postulating that the plume is expanded into a vacuum, ignoring the fact that the altitude chamber always runs at finite back pressure [7].

The primary objective of this paper is to apply both steady state and transient numerical modeling to the chemically reacting flowfield to address the issue to improve engine performance prediction. Current analyses focus on the effects of unsteady, large-scale mixing in the reacting shear layer along the chamber wall in order to understand the physics of underpredictions for thrust and specific impulse. Simultaneous emphasis on the impact of finite altitude chamber pressure on the near plume flowfield is also discussed.

The numerical algorithm is based on extending earlier supersonic reacting flow calculations [8-10] to subsonic combustion problems [11,12]. The analysis uses a three-dimensional, finite volume Navier Stokes procedure that includes chemical non-equilibrium effects. The equations can be written in a generalized coordinate system as :

$$\frac{\partial(VQ)}{\partial t} + \frac{\partial(E - E_v)}{\partial \xi} + \frac{\partial(F - F_v)}{\partial \eta} + \frac{\partial(G - G_v)}{\partial \zeta} = VH \quad (1)$$

where  $Q = (\rho, \rho u, \rho v, \rho w, e, \rho Y_i)^T$  is the vector of primary dependent variables, and  $E, F,$  and  $G$  are the inviscid flux vectors, and  $E_v, F_v,$  and  $G_v$  the viscous flux vectors in the  $\xi, \eta$  and  $\zeta$  directions, respectively. The vector  $H$  represents the source terms associated with chemical reactions and  $V$  is the cell volume.

Numerical computation for steady flow is achieved by an implicit time-marching algorithm using an LU approximate factorization in time and flux split upwinding differencing in space. The time-accurate calculation for unsteady flow is conducted by a dual time stepping procedure [13]. The finite rate chemical reaction model used in the present work for gaseous hydrogen-oxygen combustion [9], involves nine chemical species and eighteen elementary reactions. Both two-dimensional and three-dimensional formulations are available.

## RESULTS:

Detailed flowfield analyses of the combustion chamber, nozzle and near plume region for Aerojet auxiliary thruster [1-4] are presented. For the purpose of experimental measurements, the thruster has both a full nozzle (expansion ratio about 30 to 1) and a shortened nozzle (expansion ratio about 1.5 to 1). The engine throat diameter is 1.27 cm (0.5 in). Hydrogen fuel is used for both regenerative and wall film cooling (specified as percent fuel-film cooling, or % FFC). The fuel which is not used for wall cooling mixes with the oxidizer and is then ignited by a spark plug. The present computational domain starts downstream of the spark plug insert, assuming complete combustion for the core flow. The designed baseline operating conditions for the Aerojet auxiliary thruster are given by an overall oxidizer to fuel ratio of 7.71, 60.9 FFC while hydrogen film is injected at about 670 K into the combustion chamber. The total propellant mass flow rate of the baseline operating condition is 0.03435 kg/s, with oxidizer and fuel mass flow rates 0.0304 kg/s and 0.00395 kg/s, respectively. The measured chamber pressure is 524 KPa.

Mach number contours for the Aerojet cutoff nozzle are given in Figure 1. This nozzle is cutoff at an area ratio of about 1.5 to 1 to provide a sufficient number density of the major chemical species for the measurement by means of a Raman scattering technique. The upper portion of the figure demonstrates the plume profile for the altitude chamber at 1 KPa pressure while the lower portion shows plume expansion into a vacuum to compare with previous research [7]. During the experiment, a build-up finite test chamber pressure ranging from 1 to 5 KPa is detected. finite altitude chamber pressure pushes the shear layer inwards, but the computational results in the supersonic core region for expansion to vacuum and finite back pressure calculations are identical. The experimental traverse line for data taking does however extend across the plume boundary for the finite back pressure, so including back pressure effect is necessary. The cutoff nozzle plume under 1 KPa back pressure is still underexpanded.

Results of the combustor-nozzle-plume calculation of the Aerojet full nozzle thruster are given in Figure 2. The upper part shows the predicted Mach number contours while lower part shows the pressure contours, both plots are for expansion to 1 KPa altitude chamber pressure. Each Mach number contour line represents a 0.5 increment. Pressure contours are plotted on a logarithmic scale, with the pressure on each contour line being essentially 10 % lower than the previous one. Inside the combustor the pressure is nearly constant, but decreases rapidly as the flow accelerates through the nozzle. An oblique shock wave can be observed from both pressure and Mach number contours, which is a result of the flow experiencing continuous compression through the bell-shaped nozzle. The exhausted plume is nearly perfectly expanded and a shear layer is formed at the plume boundary under 1 KPa test chamber pressure.

Representative solutions of the unsteady, reactive mixing shear layer inside the combustor are given in Figure 3 and Figure 4. Figure 3 shows the spatial variation of OH radical concentration and temperature contours in the combustor. Time-accurate, unsteady calculations indicate that unsteady flow exists in the mixing layer between the heavier hot core gas and lighter hydrogen cooling film. Because of the presence of the injector base region which divides the core gas and hydrogen cooling film, large-scale vortices are shed from the base region and causes unsteady mixing in the reacting shear layer. Vortex roll-up is, however, minimized by the proximity of the combustor wall. The core flow enters the combustor at 2950 K while the hydrogen film flows along the wall at 670 K. The core gas temperature remains almost constant in the combustor. A large temperature gradient is also observed in the reacting shear layer. The temperature first increases to a peak of 3450 K because of the presence of a diffusion flame between the core gas and the cooling layer, then decreases to the coolant film temperature. The OH radical concentration is here used as an indicator of the location of the diffusion flame. It has very high concentration in the flame zone and diminishes quickly outside the flame zone. In Figure 3, the OH concentration is about 6 % in the preburned hot core gas, then rises to 16 % in the shear layer which confirms the location of the diffusion flame and finally decreases to zero in the wall cooling layer.

Figure 4 shows the temporal fluctuations of the OH concentration at several points lying across the mixing layer. Symbols in Figure 3 denote where the OH radical concentration samples are taken in the unsteady mixing layer. At the lower edge of the shear layer (symbol a), the OH concentration is constant. In the shear layer, the OH radical concentrations are plotted at three traverse stations (symbols b,c,d). It is observed that OH starts to fluctuate on different levels with respect to time at all three locations. Near the wall, in the hydrogen coolant film (symbol e), OH concentration remains nearly zero at all times.

Efforts centering on the time-averaged mixing and its impact on improving engine performance are currently underway. The predicted unsteadiness of the coolant layer and the three-dimensional nature of the

mixing layer on enhanced mixing, combustion processes, and wall cooling will also be assessed. Additional comparisons with counterpart experiments will be made.

#### REFERENCES:

- [1] Reed,B.D., Penko,P.F., Schneider,S.J. and Kim,S.C., "Experimental and Analytical Comparison of Flowfields in a 110 N (25 lbf)  $H_2/O_2$  Rocket", AIAA Paper 91-2283, 1991, Sacramento, CA.
- [2] de Groot,W. and Weiss,J.M., "Species and Temperature Measurement in  $H_2/O_2$  Rocket Flow Fields by Means of Raman Scattering Diagnostics", AIAA Paper 92-3353, 1992, Nashville, TN.
- [3] Zupanc,F.J. and Weiss,J.M., "Rocket Plume Flowfield Characterization Using Laser Rayleigh Scattering", AIAA Paper 92-3351, 1992, Nashville, TN.
- [4] Arrington,L.A. and Reed,B.D., "Performance Comparison of Axisymmetric and Three-Dimensional Hydrogen Film Coolant Injection in a 110 N Hydrogen/Oxygen Rocket", AIAA Paper 92-3390, 1992, Nashville, TN.
- [5] Weiss,J.M. and Merkle,C.L., "Numerical Investigation of Reacting Flowfields in Low-Thrust Rocket Engine Combustor", AIAA Paper 91-2080, 1991, Sacramento, CA.
- [6] Weiss,J.M.,Daines,R.L. and Merkle,C.L., "Computation of Reacting Flowfields in Low-Thrust Rocket Engines", AIAA Paper 91-3557, 1991, Cleveland, OH.
- [7] Weiss,J.M. and Merkle,C.L., "Prediction of Engine and Near-Field Plume Reacting Flows in Low-Thrust Chemical Rockets", AIAA Paper 93-0237, 1993, Reno, NV.
- [8] Shuen,J.S. and Yoon,S., "Numerical Study of Chemically Reacting Flows Using a Lower-Upper Symmetric Successive Overrelaxation Scheme", AIAA Journal, Vol. 27, No. 12, pp.1752-1760, 1989.
- [9] Yu,S.T.,Tsai,Y-L.P. and Shuen,J.S., "Three-Dimensional Calculations of Supersonic Reacting Flows Using a LU Scheme", AIAA Paper 89-0391, 1989, Reno, NV.
- [10] Molvik,G.A. and Merkle,C.L., "A Set of Strongly Coupled Upwind Algorithms for Computing Flows in Chemical Non-Equilibrium", AIAA Paper 89-0199, 1989, Reno, NV
- [11] Venkateswaran,S.,Weiss,J.M.,Merkle,C.L. and Choi,Y.-H., "Propulsion-Related Flowfields Using the Preconditioned Navier-Stokes Equations", AIAA Paper 92-3437, 1992, Nashville, TN.
- [12] Tsuei,H.-H. and Merkle,C.L., "Heat Release and Molecular Weight Effects in Shear Layer", AIAA Paper 94-0553, to be presented at AIAA Aerospace Sciences Meeting, Reno, 1994.
- [13] Shuen,J.-S., Chen,K.-H. and Choi,Y., "A Time-Accurate Algorithm for Chemical Non-Equilibrium Viscous Flows at All Speeds", AIAA Paper 92-3639, 1992, Nashville, TN.

Figure 3. Instantaneous Contour Plots of the OH Radical

Concentration and Temperature.

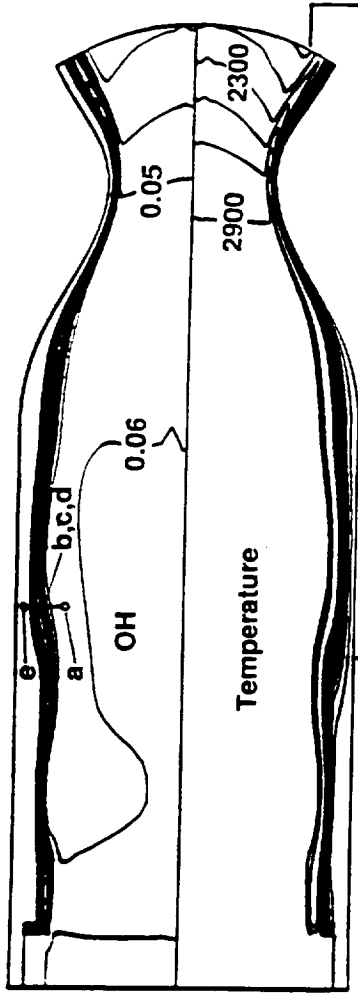


Figure 1. Mach Number Contours for Aerojet Cutoff Nozzle.

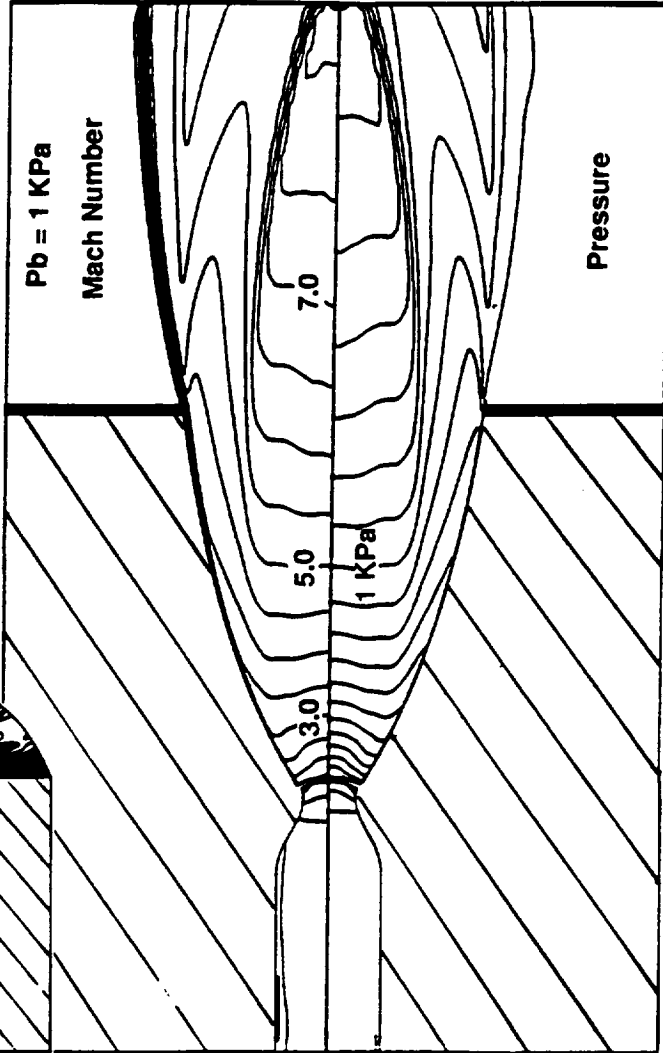
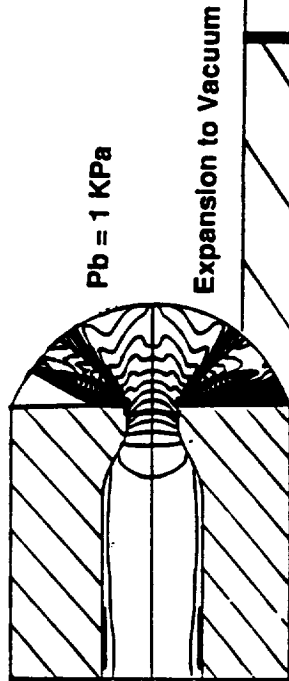


Figure 2. Mach Number and Pressure Contours for Aerojet Full Nozzle.

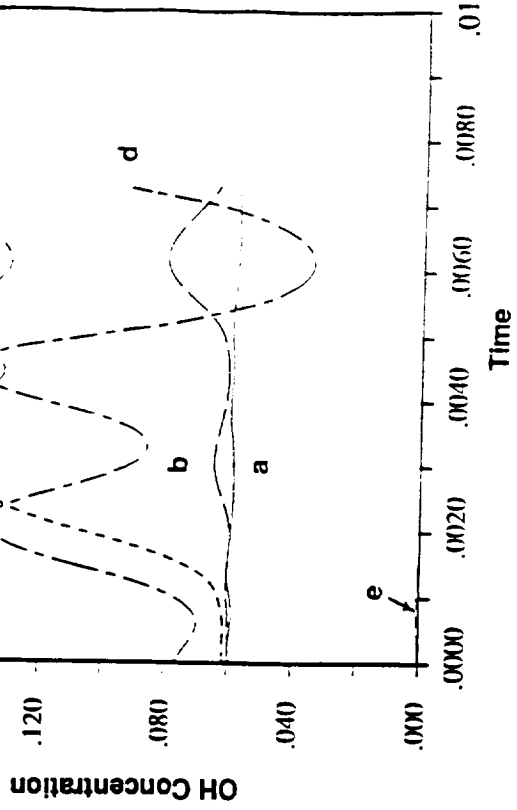


Figure 4. Temporal Variations of the OH Radical Concentration across the Mixing Layer.